Available online at www.sciencedirect.com
SCIENCE DIRECT®
Journal of Solid State Chemistry 178 (2005) 811–818
JOURNAL OF SOLID STATE CHEMISTRY
www.elsevier.com/locate/jssc

Novel protonated and hydrated $n = 1$ Ruddlesden–Popper phases, $H_xNa_{1-x}LaTiO_4 \cdot yH_2O$, formed by ion-exchange/intercalation reaction

Shunsuke Nishimoto, Motohide Matsuda, Michihiro Miyake*

Faculty of Environmental Science and Technology, Department of Environmental Chemistry and Materials, Okayama University, Tsushima-Naka, Okayama 700-8530, Japan

Received 11 June 2004; received in revised form 14 December 2004; accepted 21 December 2004

Abstract

New derivatives of layered perovskite compounds with H_3O^+ ions, H^+ ions and water molecules in the interlayer, $H_xNa_{1-x}LaTiO_4 \cdot yH_2O$, were successfully synthesized by an ion-exchange/intercalation reaction with dilute HCl solution, using an $n = 1$ member of Ruddlesden–Popper phase, $NaLaTiO_4$. Powder X-ray diffraction revealed that the layered structure changed from space group $P4/nmm$ with $a = 3.776(1)$ and $c = 13.028(5)$ Å to $I4/mmm$ with $a = 3.7533(3)$ and $c = 28.103(4)$ Å after the ion-exchange/intercalation reaction at pH 5. The change of space group indicates that the perovskite layers are transformed from staggered to an eclipsed configuration through the ion-exchange/intercalation reaction. Thermogravimetric analysis and high-temperature powder X-ray diffraction suggested the existence of the secondary hydrated phase by dehydrating $H_xNa_{1-x}LaTiO_4 \cdot yH_2O$ at 100 °C.

Keywords: Layered perovskite; Ruddlesden–Popper phase; Ion-exchange; Intercalation; Hydration

1. Introduction

It is known that there are three kinds of ion-exchangeable layered perovskites as follows: a Dion–Jacobson (D–J) family [1,2], a Ruddlesden–Popper (R–P) family [3,4], and an Aurivillius family [5] are generated as $A'[A_{n-1}B_nO_{3n+1}]$ (A', A = alkali, alkaline or rare earth and B = transition metal), $A_2'[A_{n-1}B_nO_{3n+1}]$, and $Bi_2O_2[A_{n-1}B_nO_{3n+1}]$, where $[A_{n-1}B_nO_{3n+1}]$ is the perovskite-type layer, respectively. These families have attracted considerable attention because of their interesting properties such as superconductivity [6], colossal magnetoresistance [7], etc. In recent years, the intensive study on the modification of the layered perovskites to improve their properties has been performed by soft-chemical reactions such as ion-exchange [8–10], intercalation [11], exfoliation [11], topochemical dehydration [12,13], and reductive transformation to higher members [14,15].

The intercalation of water molecules in the interlayer is an interesting reaction from the standpoint of developing new compounds. For example, water molecules intercalated in the interlayer space of $K_2Ln_2Ti_3O_{10}$ (Ln = lanthanide), which is a R–P phase, play an important role in the photocatalytic decomposition of water [16]. The proton conduction through the hydrogen-bonding network produced by intercalating water molecules in the interlayer appears in $HLa_2NbTi_2O_{10} \cdot 1.5H_2O$, which is a D–J phase [17]. Furthermore recently superconductivity was newly found in a layered $Na_{0.7}CoO_2$ via a soft-chemical route involving hydration [18].

The $n = 1$ R–P phase $NaLnTiO_4$ (Ln = lanthanide), consisting of (a) TiO_6 octahedral layers, (b) Na interlayers and (c) LaO_9 polyhedral layers ordered with

*Corresponding author. Fax: +81 86 251 8906.
E-mail address: mmiyake@cc.okayama-u.ac.jp (M. Miyake).

0022-4596/$ - see front matter © 2005 Elsevier Inc. All rights reserved.
doi:10.1016/j.jssc.2004.12.033

a sequence of –(a)–(b)–(a)–(c)–(a)– along the *c*-axis [19–21], is an interesting target for the intercalation research of water molecules. It was reported that when water molecules were intercalated in the interlayer of $NaEuTiO_4$, the shift of the perovskite slabs toward the ⟨1 1 0⟩ direction occurred along the ion-exchangeable interlayer gallery [22]. However, there are few reports on the intercalation of water molecules in series of $NaLnTiO_4$ and R–P phases with smaller alkali cations than K^+ ions located in the interlayer space. Thus, we are interested whether the intercalation of water molecules occurs in $NaLnTiO_4$ compound such as $NaLaTiO_4$, $NaNdTiO_4$, and $LiLaTiO_4$, etc. On the other hand, the crystal structure of $NaLnTiO_4$ was reported to be dependent on the size of Ln^{3+} ions as follows [19]. $NaLnTiO_4$ (Ln = La–Nd) compound crystallizes in the tetragonal symmetry with the ideal TiO_6 octahedral connections. On the other hand, $NaLnTiO_4$ (Ln = Sm–Lu) compound crystallizes in the orthorhombic symmetry with the mutual tilting of TiO_6 octahedra, which brings the stronger interaction between the TiO_6 octahedron and Na^+ ion than that in the tetragonal. Therefore, the hydration behaviors of the tetragonal compounds such as $NaLaTiO_4$, $NaNdTiO_4$ and $LiLaTiO_4$, etc. are expected to be different from those of the orthorhombic compounds such as $NaSmTiO_4$ and $NaEuTiO_4$, if the intercalation of water molecules occurs in the tetragonal compounds.

Furthermore, it was reported that the hydrated phases, $HLaTiO_4 \cdot xH_2O$, were prepared by the ion-exchange reaction of Na^+ ions in $NaLaTiO_4$ using HNO_3 solution of pH 1 [23]. This suggests that the ion-exchange reaction of $NaLaTiO_4$ leads the intercalation of water molecules. Therefore, the formation of new derivatives such as $H_xA_{1-x}LaTiO_4 \cdot yH_2O$ (A = alkali) is expected by changing the ion-exchange ratio of Na^+ ions in $NaLaTiO_4$ to H^+ ions. In addition, the systematic investigation concerning the ion-exchange ratio in $NaLaTiO_4$ could reveal the relation between the ion-exchange and intercalation behaviors.

With such a background, the intercalation of water molecules in the interlayer of $NaLaTiO_4$, $LiLaTiO_4$ and $KLaTiO_4$ has been investigated, using HCl solutions with various pH values. Consequently, the new derivatives of $n = 1$ hydrated and anhydrous R–P phases were successfully prepared. In this paper, we describe the syntheses of hydrated phases, $H_xNa_{1-x}LaTiO_4 \cdot yH_2O$, by the ion-exchange/intercalation reactions of $NaLaTiO_4$, and the characterization of resulting materials. In addition, the ion-exchange/intercalation reaction of $NaLaTiO_4$ is compared with those of $LiLaTiO_4$ and $KLaTiO_4$.

2. Experimental

The starting compound, $NaLaTiO_4$, was prepared by the conventional solid-state reaction [19–21]. Prior to the preparation, La_2O_3 was predehydrated at 900 °C for 9 h, because La_2O_3 agent contains a small amount of $La(OH)_3$. The stoichiometric amounts of TiO_2 and La_2O_3 and 50% excess of Na_2CO_3 were mixed, and heated at 900 °C for 30 min after preheating at 700 °C for 2 h in the air. The product was washed with distilled water and dried at 160 °C. The preparations of $LiLaTiO_4$ and $KLaTiO_4$ were performed by ion-exchange reactions of the parent $NaLaTiO_4$ in molten $LiNO_3$ and CH_3COOK in 300–330 °C for 3 d, respectively [24]. During the ion-exchange reaction, the molten salt was refreshed everyday. The products were washed with distilled water, and dried at 160 °C. The prepared $KLaTiO_4$ was heated at 500 °C to form anhydrous phase prior to the ion-exchange/intercalation reactions, because it is easily hydrated in the air [25].

The ion-exchange/intercalation reactions for $NaLaTiO_4$, $LiLaTiO_4$ and $KLaTiO_4$ were carried out in HCl solutions in pH 1–5 at room temperature for several days. The HCl solution was refreshed everyday during the reaction. The different amounts of specimen were used in the reactions to accurately detect the pH change of the solution. The resulting samples were washed with distilled water and dried at room temperature.

Powder X-ray diffraction (XRD) patterns were measured on a Rigaku RINT2100/PC diffractometer with monochromated Cu$K\alpha$ radiation at room and elevated temperatures. Energy-dispersive X-ray emission analysis (EDX) was performed on a JEOL JSM-6300 instrument. The ion-exchange ratios were determined by measuring pH value and A^+ (A = Li, Na, and K) ion concentration in filtrates, using a TOA HM-5S pH meter and a Shimadzu AA6800F atomic absorption spectrometer, respectively. ^{1}H magic-angle spinning nuclear magnetic resonance (MAS NMR) spectra were recorded at room temperature, using a Varian ^{UNITY}INOVA300FT NMR spectrometer operating at a nominal frequency of 300 MHz. The sample spinning speed at the magic angle to the external field was 6.0 kHz. Thermogravimetric analysis (TGA) was performed on a Rigaku TAS100 instrument at a heating rate of 10 °C min^{-1} in the air.

3. Results and discussion

3.1. Syntheses and characterization of $H_xNa_{1-x}LaTiO_4 \cdot yH_2O$

The XRD revealed that the compound prepared by solid-state reaction was identified as $NaLaTiO_4$, and contained no impurities, referring to the previous descriptions [19–21]. Thus, the resulting material was employed in the following experiments as a starting compound.

The ion-exchange/intercalation reactions for $NaLaTiO_4$ were conducted, using HCl solutions in pH 1–5. The pH value and Na^+ ion concentration of the solution increased during the contact with $NaLaTiO_4$, suggesting that an ion-exchange reaction proceeded. The exchange ratio of Na^+/H^+ was estimated to be about 1.0 from the pH change and analytical results by the atomic absorption. Fig. 1 shows the time dependences of the released ratio of Na^+ ions from $NaLaTiO_4$ for the reactions with HCl solutions in pH 1–5. The released ratio of Na^+ ions from $NaLaTiO_4$ attained 100% within 12 h at pH 1, and Na^+ ions in $NaLaTiO_4$ were completely exchanged with H^+ ions, as seen in the previous report [23]. On the other hand, the ion-exchange reactions gradually proceeded and their ratios decreased with increasing initial pH value. The ion-exchange reactions in pH 3–5 were especially remarkable, and the aspects of these reactions were similar to one another. The ion-exchange reactions in pH 2–5 were incomplete, although the reaction solutions were refreshed every day. These were also supported by the EDX analyses of the resulting materials within the standard error of 5%.

Fig. 2 shows XRD patterns of $NaLaTiO_4$ before and after the treatments in pH 1–5. The XRD revealed that the products by the treatments at pH 1 for 12 h and pH 2 for 24 h were isostructural with $NaLaTiO_4$, which belongs to space group $P4/nmm$, and these XRD peaks corresponding to the basal spacing shifted towards the higher diffraction angle (2θ) side, compared with $NaLaTiO_4$. The resulting materials at pH 1 and 2 were, therefore, decided as anhydrous $HLaTiO_4$ and anhydrous $H_{0.83}Na_{0.17}LaTiO_4$, respectively, referring to the results by the atomic absorption and EDX analyses, together with the previous paper [23]. On the other hand, the XRD patterns of the products by the

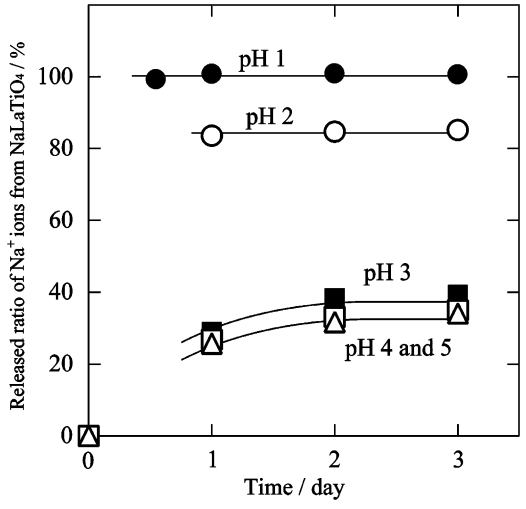

Fig. 1. Time dependences of the released ratio of Na^+ ions from $NaLaTiO_4$ treated with HCl solutions in pH 1–5.

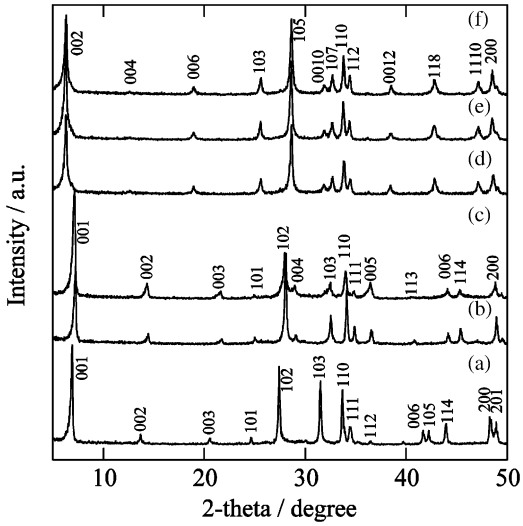

Fig. 2. XRD patterns of $NaLaTiO_4$ (a) before and after HCl treatments (b) at pH 1 for 12 h, (c) at pH 2 for 24 h, (d) at pH 3 for 48 h, (e) at pH 4 for 48 h and (f) at pH 5 for 48 h.

treatments in pH 3–5 for 48 h could not be indexed as the space group $P4/nmm$ but $I4/mmm$ with the double basal spacing of $HLaTiO_4$. Moreover, the XRD peaks corresponding to the basal spacing shifted towards the lower 2θ side, indicating that water molecules were intercalated into the interlayer space.

^1H MAS NMR spectra were measured to confirm the existence of the proton and water of crystallization in the specimens. The products at pH 1 and 2 were heated at 100 °C before the measurement to remove the adsorbed water on the surface. No significant difference between the XRD patterns before and after the heat treatment could be observed. A single peak was observed on the spectra of the products at pH 1 and 2, whereas four peaks were observed on the spectra of the products at pH 3–5. Fig. 3 shows ^1H MAS NMR spectra of the products at pH 1 and 5. The peak of the product at pH 1 was sharp and chemically shifted by 12.2 ppm with respect to TMS as a reference. The high chemical shift (~9 ppm) implies that the electron density of the hydrogen in the product is relatively low [26]. That is, the proton was considered to exist in the product at pH 1. On the other hand, a strong peak at 7.9 ppm and three weak peaks at 11.2, 6.3 and 1.3 ppm were observed on the spectrum of the product at pH 5. It is known that hydrogens belonging to structural OH^- groups exhibit resonances in two different chemical shift ranges; 4.2–5.0 and 6.8–8.0 ppm [17]. Therefore, the peak at 7.9 ppm may arise from OH^- in the water of crystallization. Furthermore, the peak at 11.2 ppm suggests the existence of the proton (H^+) in analogy with the product at pH 1. Consequently, it was revealed that the product at pH 5 contained the proton and water of crystallization. The peaks at 6.3 and 1.3 ppm were

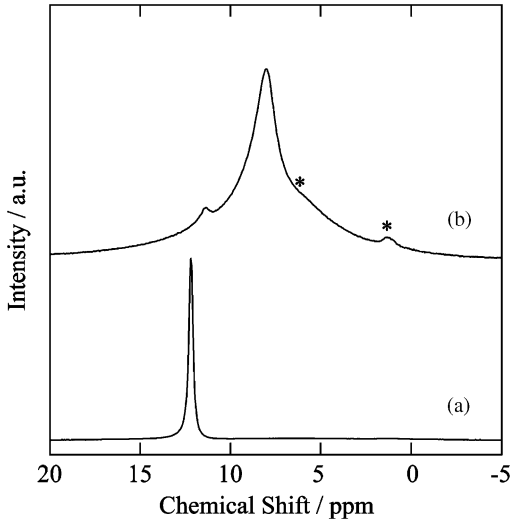

Fig. 3. ^{1}H MAS NMR spectra of $NaLaTiO_4$ after the treatment (a) at pH 1 for 12 h and (b) at pH 5 for 48 h. The asterisks represent the peaks assigned to the water adsorbed on the surface.

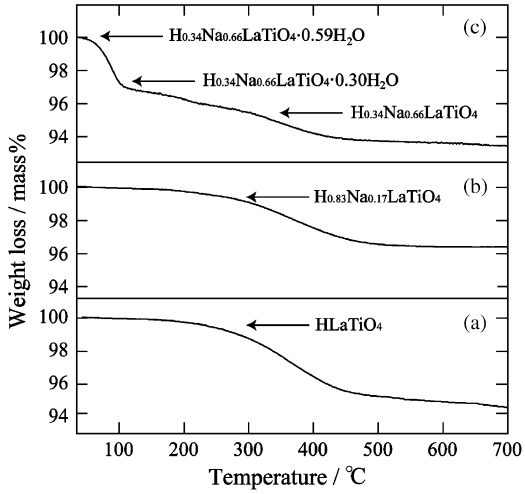

Fig. 4. TG curves of (a) $HLaTiO_4$, (b) $H_{0.83}Na_{0.17}LaTiO_4$ and (c) $H_{0.34}Na_{0.66}LaTiO_4 \cdot 0.59H_2O$.

assigned to the adsorbed water on the surface, because peaks at 6.3 and 1.3 ppm as well as a peak at 12.2 ppm appeared on the spectrum of the product at pH 1 without heating at 100 °C. The amount of the adsorbed water in the product at pH 5 was estimated to be about 8 mass% of the total water contents from the peak areas at 7.9, 6.3 and 1.3 ppm.

The thermal analyses were performed to estimate amounts of intercalated water molecules and confirm the contents of loaded protons. One-step weight loss above 300 °C was observed on the TG curves of the products at pH 1 and 2, whereas three-step weight losses including the weight loss above 300 °C were observed on the TG curves of the products in pH 3–5. Fig. 4 representatively shows the TG curves of the products at pH 1, 2 and 5. The products at pH 1 and 2 were preheated at 100 °C before the measurements to remove the adsorbed water on the surface, referring the results of the ^{1}H MAS NMR measurement. The weight losses above 300 °C observed in the products at pH 1 and 2 were assigned as corresponding to the elimination of H_2O produced by the interlayer proton and oxygen of perovskite layer, according to the reaction; $H_xNa_{1-x}LaTiO_4 \rightarrow Na_{1-x}LaTiO_{4-1/2x} + 1/2x\ H_2O$, since the experimental weight losses for pH 1 and 2 were consistent with the theoretical ones estimated from the proton contents based on the analytical results, respectively. The behavior of the weight loss above 300 °C observed in the product at pH 5 was similar to those at pH 1 and 2. Thus, it was assumed that the weight loss above 300 °C was due to the elimination of H_2O produced by the interlayer proton and oxygen of perovskite layer, while the weight loss below 300 °C was due to the elimination of H_2O intercalated in the interlayer. Consequently, an amount of intercalated water molecules in the product at pH 5 was estimated to be averagely $0.59H_2O$ per formula from the results of the TG and ^{1}H MAS NMR measurements. Table 1 summarizes the compositions and lattice parameters based on the analytical results and XRD data of all the products.

The high-temperature XRD patterns were measured to examine the dehydration process of $H_{0.34}Na_{0.66}LaTiO_4 \cdot 0.59H_2O$ obtained by the reaction for 48 h at pH 5, as shown in Fig. 5. The XRD pattern at 100 °C could be indexed as space group $P4/nmm$ with $a = 3.746(4)$ and $c = 12.99(3)$ Å, although a small amount of $H_{0.34}Na_{0.66}LaTiO_4 \cdot 0.59H_2O$ with the space group $I4/mmm$ barely remained, suggesting the formation of the secondly hydrated phase, whose composition was estimated to be $H_{0.34}Na_{0.66}LaTiO_4 \cdot 0.30H_2O$ from the TG curve.

Interestingly, the XRD pattern of $H_{0.34}Na_{0.66}LaTiO_4 \cdot 0.30H_2O$ was similar to those of the intermediates, which appeared in the ion-exchange/intercalation reactions in pH 3–5. Fig. 6 shows the XRD patterns of $NaLaTiO_4$ before and after the treatments at pH 5 for 24 and 48 h. The XRD pattern after the treatment for 24 h could be indexed as space group $P4/nmm$ with $a = 3.751(1)$ and $c = 12.91(1)$ Å, and seemed almost identical to that of $H_{0.34}Na_{0.66}LaTiO_4 \cdot 0.30H_2O$ observed at 100 °C. Moreover, thermal analysis of the product at pH 5 for 24 h showed the presence of the intermediate phase. Fig. 7 shows the TG curves of the products at pH 5 for 24 and 48 h. Both the curves above 100 °C were similar to each other. The analytical results suggest that the product for 24 h contained about 0.3 moles of waters and protons. Consequently, it was considered that $H_{0.34}Na_{0.66}LaTiO_4 \cdot 0.59H_2O$ was formed via the formation of the intermediate phase

Table 1
Compositions and lattice parameters of the products by ion-exchange/intercalation reactions with HCl solutions in pH 1–5

pH	Compound	a (Å)	c (Å)
	$NaLaTiO_4$	3.776(1)	13.028(5)
1	$HLaTiO_4$	3.7186(5)	12.290(2)
2	$H_{0.83}Na_{0.17}LaTiO_4$	3.7248(5)	12.290(2)
3	$H_{0.39}Na_{0.61}LaTiO_4 \cdot 0.55H_2O$	3.7528(3)	28.114(5)
4	$H_{0.35}Na_{0.65}LaTiO_4 \cdot 0.55H_2O$	3.7528(3)	28.114(5)
5	$H_{0.34}Na_{0.66}LaTiO_4 \cdot 0.59H_2O$	3.7533(3)	28.103(4)

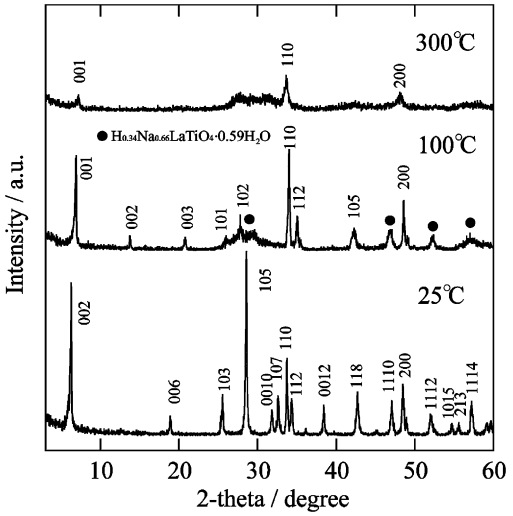

Fig. 5. XRD patterns of $H_{0.34}Na_{0.66}LaTiO_4 \cdot 0.59H_2O$ as a function of temperature.

such as $H_{0.34}Na_{0.66}LaTiO_4 \cdot 0.30H_2O$ in the ion-exchange/intercalation reaction at pH 5. In addition, it was noteworthy that the number of loaded protons was approximately same as that of water molecules in $H_{0.34}Na_{0.66}LaTiO_4 \cdot 0.30H_2O$. This result and the thermal analysis suggest that $H_{0.34}Na_{0.66}LaTiO_4 \cdot 0.30H_2O$ was formed as the intermediate by the ion-exchange reaction of Na^+ ions in $NaLaTiO_4$ with H_3O^+ ions as well as a few H^+ ions in the reaction solution.

The XRD pattern heated at 300 °C, as seen in Fig. 5, showed the anhydrous phase $H_{0.34}Na_{0.66}LaTiO_4$ with low crystallinity. The lowering of crystallinity may be due to the partial elimination of H_2O produced by the interlayer proton and oxygen of perovskite layer, which lead the formation of the A-site defective $n = 2$ R–P phase $La_2\square Ti_2O_7$ with the low crystallinity caused by the disorder [12].

On the basis of these results, the models of structural change by the ion-exchange/intercalation reactions are demonstrated in Fig. 8. The H^+ ion concentration in the reaction solution controls whether hydration occurs. That is, many Na^+ ions are immediately exchanged with H^+ ions by the concentration slope of H^+ ion at the interface between $NaLaTiO_4$ and the solutions at

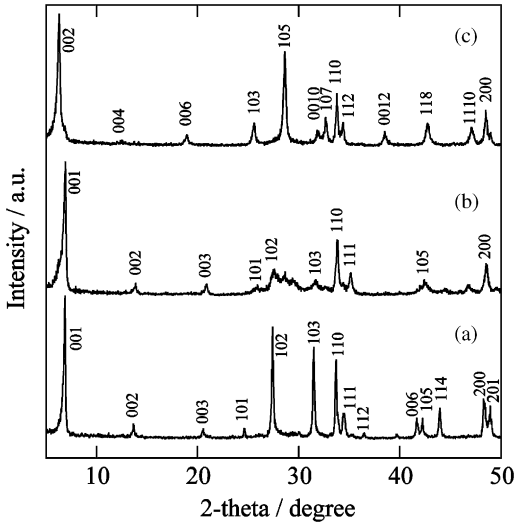

Fig. 6. XRD patterns of $NaLaTiO_4$ (a) before and after HCl treatments at pH 5 for (b) 24 h and (c) 48 h.

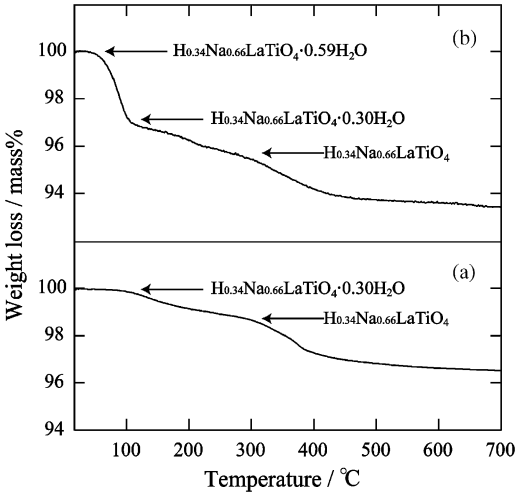

Fig. 7. TG curves of (a) $H_{0.34}Na_{0.66}LaTiO_4 \cdot 0.30H_2O$ and (b) $H_{0.34}Na_{0.66}LaTiO_4 \cdot 0.59H_2O$.

pH 1 and 2. Then, the exchange reaction leads the c-axis to the shrinkage, because the protons smaller than Na^+ ions occupy the interlayer space, and results in the formation of $H_xNa_{1-x}LaTiO_4$ (Fig. 8(b)), which is isostructural with $NaLaTiO_4$. The further intercalation could not occur because of the narrow interlayer space. That is, the intercalation of water molecules does not occur in pH $\leqslant$ 2. This behavior was different from the previous report on the $HLaTiO_4 \cdot xH_2O$ [23]. The difference between the present and the previous studies is probably caused by the difference of the experimental procedure, e.g., the washing treatment of $NaLaTiO_4$.

On the other hand, Na^+ ions in $NaLaTiO_4$ are slowly exchanged with H_3O^+ ions and a few H^+ ions in pH $\geqslant$ 3, because the concentration slope of H^+ ion at the

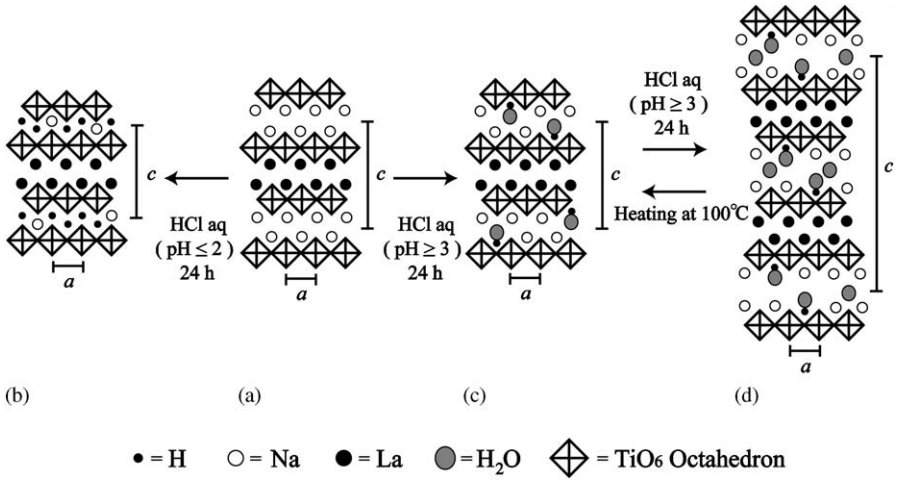

Fig. 8. Illustration of structural change induced by ion-exchange/intercalation reactions in $NaLaTiO_4$.

interface between $NaLaTiO_4$ and the solutions in pH ⩾ 3 was too small to form $H_xNa_{1-x}LaTiO_4$ with the narrow interlayer space. Then, $H_{0.34}Na_{0.66}LaTiO_4 \cdot 0.30H_2O$ is formed without structural change at first stage (Fig. 8(c)). The behavior observed was different from the hydration behavior of $NaEuTiO_4$, in which the Na^+ ions are not exchanged. This could be explained by the difference of the structures between $NaLaTiO_4$ and $NaEuTiO_4$ as follows. $NaLnTiO_4$ compound (Ln = La–Nd) crystallizes in the tetragonal with the ideal TiO_6 octahedra connections, because Ln–O bond lengths match with Ti–O bond lengths along the a-axis, and TiO_6 octahedra are weakly bonded to Na^+ ions. On the other hand, the mismatch between Ln–O lengths and Ti–O lengths was induced when the size of Ln^{3+} ion is reduced less than that of Nd^{3+} ion [19]. As a result, the TiO_6 octahedra mutually tilt to stabilize the structure, and are strongly bonded to Na^+ ions. It was, therefore, considered that the weak interaction between the perovskite layers and interlayer Na^+ ions, compared with that of $NaEuTiO_4$, could not inhibit the elimination of the Na^+ ions from $NaLaTiO_4$ at even the low H^+ ion concentration, and thus allowed the ion-exchange/intercalation reactions.

Furthermore, the water molecules can be intercalated in the interlayer at the next stage (Fig. 8d), because the interlayer space of the intermediates obtained in pH ⩾ 3 was wider than those of $HLaTiO_4$ and $H_{0.83}Na_{0.17}LaTiO_4$. It is considered that the interlayer ion hydration energy promotes the hydration reaction as the driving force, as seen in the previous report on the hydration in clay minerals [27]. The space group of the resulting compound, $H_{0.34}Na_{0.66}LaTiO_4 \cdot 0.59H_2O$, is changed from $P4/nmm$ to $I4/mmm$ by the intercalation of water molucules. This indicates that the perovskite layers shift toward the ⟨1 1 0⟩ direction and results in eclipsed rather than a staggered configuration, as seen in previous reports on $K_2La_2Ti_3O_{10} \cdot H_2O$ [8] and $NaEuTiO_4 \cdot 0.5H_2O$ [22]. $H_{0.34}Na_{0.66}LaTiO_4 \cdot 0.59H_2O$ is transformed into $H_{0.34}Na_{0.66}LaTiO_4 \cdot 0.30H_2O$ with the structural change from $I4/mmm$ to $P4/nmm$ by the heat treatment at 100 °C.

3.2. Syntheses of $H_xA_{1-x}LaTiO_4 \cdot yH_2O$ (A = Li and K)

The ion-exchange/intercalation reactions for $ALaTiO_4$ (A = Li and K), which has the layered structure similar to $NaLaTiO_4$, were also examined. The EDX analyses indicated the formations of $LiLaTiO_4$ and $KLaTiO_4$ by the ion-exchange reactions of $NaLaTiO_4$ in molten salts. The XRD pattern of $LiLaTiO_4$ was indexed as the tetragonal $P4/nmm$ with $a = 3.7752(4)$ and $c = 12.032(1)$ Å. As Li^+ ions are located at fourfold coordinate sites not at ninefold coordinate sites in $NaLaTiO_4$ [24], the c axis of $LiLaTiO_4$ is shorter than the value expected from cation size in the series of $ALaTiO_4$ (A = Li, Na, and K) compound. On the other hand, the XRD pattern of $KLaTiO_4$ was indexed as the orthorhombic $Pbcm$ with $a = 13.401(4)$, $b = 5.428(2)$, and $c = 5.466(2)$ Å. In the present study, $KLaTiO_4$ was prepared in the molten salt to compare with $LiLaTiO_4$, though it has been reportedly prepared by an ion-exchange reaction in KOH solutions [25]. The different preparation condition may cause the slight difference of the cell parameters between the previous and present studies [25].

The ion-exchange reaction of $LiLaTiO_4$ for H^+ ions proceeded with the molar ratio of $Li^+/H^+ \approx 1.0$, when $LiLaTiO_4$ contacted with the HCl solutions at pH 1 and 2. The released ratio of Li^+ ions from $LiLaTiO_4$ attained 100% at pH 1 and 69% at pH 2, respectively. Fig. 9 shows the XRD patterns of $LiLaTiO_4$ before and after the treatments at pH 1 and 2. Both the XRD

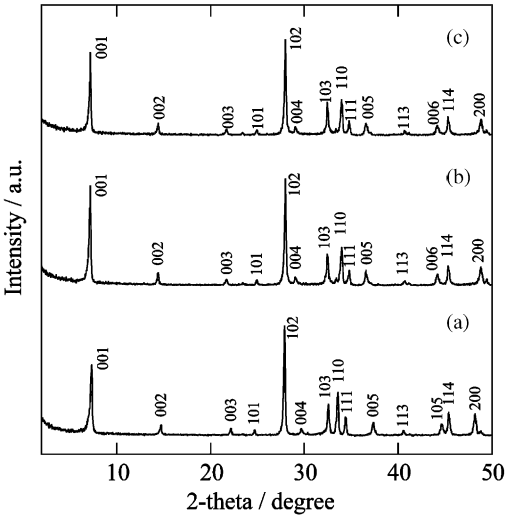

Fig. 9. XRD patterns of $LiLaTiO_4$ (a) before and after the ion-exchange reaction (b) at pH 1 for 12 h and (c) at pH 2 for 12 h.

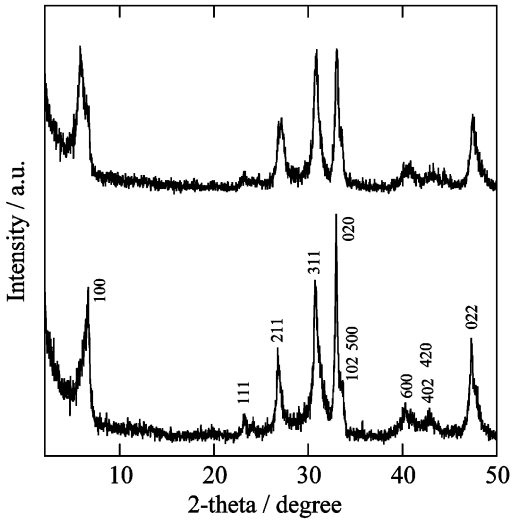

Fig. 10. XRD patterns of $KLaTiO_4$ (a) before and (b) after the intercalation reaction at pH 5 for 48 h.

patterns after the treatments were indexed as the tetragonal $P4/nmm$, and the cell dimensions estimated from the XRD pattern were $a = 3.7249(4)$ and $c = 12.289(2)$ Å for pH 1 and $a = 3.7256(5)$ and $c = 12.286(3)$ Å for pH 2, respectively. The cell dimensions for pH 1 and 2 were in agreement with each other. The TGA revealed that there were no water molecules intercalated in the resulting materials. The chemical compositions of the materials obtained at pH 1 and 2 were, therefore, determined to be $HLaTiO_4$ and $H_{0.69}Li_{0.31}LaTiO_4$, respectively. On the other hand, Li^+ ions were not exchanged with H^+ ions when the samples were treated with HCl solutions in pH $\geqslant$ 3. The interlayer structure different from $NaLaTiO_4$, such as the location of Li^+ ion and narrow interlayer space, probably brought the different ion-exchange ability.

The crystal structure of $KLaTiO_4$ was decomposed when $KLaTiO_4$ contacted with HCl solutions in pH $\leqslant$ 4. On the other hand, the release of K^+ ions from $KLaTiO_4$ was undetectable during the contact with HCl solution at pH 5. Fig. 10 shows the XRD patterns of $KLaTiO_4$ before and after the treatment at pH 5. The XRD pattern after the treatment was almost identical with that of hydrated $KLaTiO_4$ previously reported [25]. Furthermore, TGA showed the presence of the water molecules. Consequently, the hydrated phase was formed without the ion-exchange reactions of K^+ ions in $KLaTiO_4$ with H^+ ions. This behavior was similar to the hydrations in $NaEuTiO_4$ [22] and $K_2La_2Ti_3O_{10}$ [16].

The ion-exchange and hydration abilities of $LiLaTiO_4$ and $KLaTiO_4$ were different from each other. That is, in $LiLaTiO_4$ with tetragonal symmetry, the ion-exchange reaction with H^+ ions was observed in pH $\leqslant$ 2, but the hydration was not observed in pH 1–5. On the other hand, in $KLaTiO_4$ with orthorhombic symmetry, the ion-exchange reaction with H^+ ions was not observed in pH 1–5, but the hydration was observed at pH 5.

4. Conclusion

In this paper, we have described the preparations of the new derivatives of $n = 1$ R–P phases $H_xA_{1-x}LaTiO_4 \cdot yH_2O$ (A = Li, Na, and K) by the ion-exchange/intercalation reactions, using HCl solutions in pH 1–5. In the series of $ALaTiO_4$ (A = Li, Na, and K), some differences of the ion-exchange and hydration abilities, which were considered to be induced by the interaction between the interlayer cations and perovskite layers and the interlayer distance, were found as follow: the ion-exchange reactions of the interlayer cations with H^+ ions were observed in $LiLaTiO_4$ and $NaLaTiO_4$ with tetragonal symmetries. Consequently, $H_xA_{1-x}LaTiO_4$ (A = Li, and Na) was formed by the treatments at pH 1 and 2, and the ion-exchange ratio depended on the initial pH value. On the other hand, the ion-exchange reaction was not observed in $KLaTiO_4$ with orthorhombic symmetry. The ion-exchange reaction and hydration occurred in $NaLaTiO_4$ in pH $\geqslant$ 3, whereas the hydration occurred in $KLaTiO_4$ at pH 5 and did not occur in $LiLaTiO_4$ in pH 1–5. The formation of the hydration in $NaLaTiO_4$ proceeded by two steps. First, Na^+ ions in $NaLaTiO_4$ were exchanged with H_3O^+ and H^+ ions. Next, the water molecules were intercalated in the interlayer, with the structural change of the stacking perovskite layer from a staggered to an eclipsed configuration. These compounds are expected to be good photocatalysts for splitting water, referring to the previous report [16]. For the application of these compounds to functional materials, more detailed

structural characterization such as the locations of protons and water molecules in the interlayer would be challenging.

Acknowledgment

This work was partly supported by The Okayama University 21st Century COE Program "Strategic Solid Waste Management for a Sustainable Society".

References

[1] M. Dion, M. Ganne, M. Tournoux, Mater. Res. Bull. 16 (1981) 1429–1435.
[2] A.J. Jacobson, J.W. Johnson, J.T. Lewandowski, Inorg. Chem. 24 (1985) 3727–3729.
[3] S.N. Ruddlesden, P. Popper, Acta Crystallogr. 10 (1957) 538–539.
[4] S. Uma, A.R. Raju, J. Gopalakrishnan, J. Mater. Chem. 3 (1993) 709–713.
[5] B. Aurivillius, Ark. Kemi 1 (1949) 463–480.
[6] J.G. Bednorz, K.A.Z. Müller, M. Takashige, Science 236 (1987) 73–75.
[7] Y. Moritomo, A. Asamitsu, H. Kuwahara, Y. Tokura, Nature 380 (1996) 141–144.
[8] J. Gopalakrishnan, V. Bhat, Inorg. Chem. 26 (1987) 4299–4301.
[9] P.J. Ollivier, T.E. Mallouk, Chem. Mater. 10 (1998) 2585–2587.
[10] W. Sugimoto, M. Shirata, Y. Sugahara, K. Kuroda, J. Am. Chem. Soc. 121 (1999) 11601–11602.
[11] R.E. Schaak, T.E. Mallouk, Chem. Mater. 12 (2000) 3427–3434.
[12] V. Thangadurai, G.N. Subbanna, J. Gopalakrishnan, J. Chem. Commun. (1998) 1299–1300.
[13] R.E. Schaak, T.E. Mallouk, J. Solid State Chem. 155 (2000) 46–54.
[14] R.E. Schaak, T.E. Mallouk, J. Am. Chem. Soc. 122 (2000) 2798–2803.
[15] R.E. Schaak, E.N. Guidry, T.E. Mallouk, Chem. Commun. (2001) 853–854.
[16] K. Domen, J. Yoshimura, T. Sekine, A. Tanaka, T. Onishi, Catal. Lett. 4 (1990) 339–343.
[17] G. Mangamma, V. Bhat, J. Gopalakrishnan, S.V. Bhat, Solid State Ion. 58 (1992) 303–309.
[18] K. Takada, H. Sakurai, E. Takayama-Muromachi, F. Izumi, R.A. Dilanian, T. Sasaki, Nature 422 (2003) 53–55.
[19] K. Toda, Y. Kameo, S. Kurita, M. Sato, J. Alloys Compd. 234 (1996) 19–25.
[20] S.H. Byeon, S.O. Lee, H. Kim, J. Solid State Chem. 130 (1997) 110–116.
[21] W.J. Zhu, H.H. Feng, P.H. Hor, Mater. Res. Bull. 31 (1996) 107–111.
[22] K. Toda, Y. Kameo, S. Kurita, M. Sato, Bull. Chem. Soc. Jpn. 69 (1996) 349–352.
[23] S.H. Byeon, J.J. Yoon, S.O. Lee, J. Solid State Chem. 127 (1996) 119–122.
[24] K. Toda, S. Kurita, M. Sato, J. Ceram. Soc. Jpn. 104 (1996) 140–142.
[25] R.E. Schaak, T.E. Mallouk, J. Solid State Chem. 161 (2001) 225–232.
[26] E. Brunner, H.G. Karge, H. Pfeifer, Z. Phys. Chem. 176 (1992) 173–183.
[27] D.E. Smith, Y. Wang, H.D. Whitley, Fluid Phase Equilib. 222–223 (2004) 189–194.